JGR Space Physics

RESEARCH ARTICLE
10.1029/2023JA032116

Observational Characteristics of High-Latitude Ionization Trough Seen by Swarm

Su-In Kim[1], Young-Sil Kwak[2,3], Hyosub Kil[4], Jaeheung Park[2,3], and Khan-Hyuk Kim[1]

[1]School of Space Research, Kyung Hee University, Yongin, South Korea, [2]Division of Space Science, Korea Astronomy and Space Science Institute, Daejeon, South Korea, [3]Department of Astronomy and Space Science, University of Science and Technology, Daejeon, South Korea, [4]Johns Hopkins University Applied Physics Laboratory, Laurel, MD, USA

Key Points:

- Measurements of radial current from Swarm satellite provide a tool to distinguish mid- and high-latitude ionization troughs
- High-latitude troughs occur more frequently in summer than winter and in dawn/dusk sectors than the noon/midnight sectors
- High-speed plasma convection is the primary cause of high-latitude trough, and field-aligned current is a secondary contributing factor

Correspondence to:
Y.-S. Kwak,
yskwak@kasi.re.kr

Citation:
Kim, S.-I., Kwak, Y.-S., Kil, H., Park, J., & Kim, K.-H. (2024). Observational characteristics of high-latitude ionization trough seen by swarm. *Journal of Geophysical Research: Space Physics*, *129*, e2023JA032116. https://doi.org/10.1029/2023JA032116

Received 23 SEP 2023
Accepted 19 APR 2024

Abstract This study investigates the distribution and formation mechanisms of ionization troughs inside an auroral oval (referred to as high-latitude troughs) by analyzing Swarm observations from May–August 2014. Simultaneous measurements of plasma density, 3-dimensional ion velocity, ionospheric radial current (IRC), and electron temperature are available during this period. Because high-latitude troughs appear within an auroral oval while mid-latitude troughs appear at the equatorward edge of the auroral oval, the positioning of troughs relative to the equatorward auroral boundary becomes critical for distinguishing between the two types of troughs. We ascertain the auroral boundary and the orientation of field-aligned currents using IRC data derived from magnetic field measurements. The principal features of high-latitude troughs identified from Swarm data include: (a) enhancements in ion velocity and electron temperature, (b) the presence of downward or absent field-aligned current (FAC), and (c) a more frequent occurrence in the Northern (summer) Hemisphere than in the Southern (winter) Hemisphere and in the dawn and dusk sectors than in the noon and midnight sectors. The alignment of the density minimum with the velocity maximum underscores the role of high-speed plasma convection in the formation of high-latitude troughs; atmospheric frictional heating promotes the O^+ loss through dissociative recombination. The prevailing appearance of high-latitude troughs at dawn and dusk sectors, coupled with downward field-aligned currents, indicates the involvement of outward electron evacuation in trough formation.

1. Introduction

Ionization troughs in the ionospheric F-region appear as longitudinally extended structures with plasma densities significantly lower than the ambient plasma density. These troughs, observed at various latitudes, arise from distinct physical processes. There are the equatorial ionization trough, developing around the magnetic equator in association with the fountain effect (Hanson & Moffett, 1966), and the mid-latitude (or main) ionization trough, forming in the equatorward subauroral region in association with stagnant plasma flow (Knudsen, 1974; Spiro et al., 1978). These troughs are persistent ionospheric features that recurrently appear around similar times, although their intensities vary with time, season, and solar and magnetic activities. Ionization troughs also develop in high latitudes (Dudeney et al., 1982; Grebowsky et al., 1976; Muldrew, 1965). While not as pronounced as other troughs, high-latitude troughs are also persistent features that recur inside an auroral oval or polar cap regardless of geomagnetic activity.

Equatorial ionization troughs are readily distinguishable from mid- and high-latitude ionization troughs because the locations of equatorial ionization troughs are always around the magnetic equator. However, mid- and high-latitude ionization troughs (hereafter referred to as mid- and high-latitude troughs) develop within proximity to an auroral oval, and their locations vary with geomagnetic activity and time (Park et al., 2012; Yang et al., 2015). Because they are difficult to distinguish by the trough morphology or its occurrence latitude, the boundary of an auroral oval is an important factor for the distinction of mid- and high-latitude troughs; mid- and high-latitude troughs are located at lower and higher latitudes relative to the equatorward auroral boundary, respectively (Rodger et al., 1992; Voiculescu et al., 2006). As well as the locations, the generation mechanisms of the mid- and high-latitude troughs are different. Many studies investigated the morphology and generation mechanism of the mid-latitude trough using diverse ground and space-based observations (Aa et al., 2020; Anderson et al., 2008; Fu et al., 2010; He et al., 2011; Moffett & Quegan, 1983; Park et al., 2012; Spiro et al., 1978; Werner & Prölss, 1997; Whalen, 1989; Yang et al., 2015; Yizengaw et al., 2005; Yizengaw & Moldwin, 2005). The mid-latitude trough is produced at the location where the plasma flows caused by the high-latitude plasma convection and corotation

with the Earth are opposite. The stagnation in the plasma flows in the absence of photoionization results in the reduction of the oxygen ion (O^+) by dissociative recombination (Spiro et al., 1978). The increase of the dissociative recombination rate of O^+ is also one of the formation mechanisms of the high-latitude trough, but the increase of the dissociative recombination rate is caused by the frictional heating associated with high-speed plasma convection (Williams & Jain, 1986). Thus, the increase of the dissociative recombination rate in the mid- and high-latitude troughs is caused by opposite behaviors in the plasma flow. The behaviors of the ion temperature in the troughs are consistent with the behaviors of the plasma flow; the ion temperature is elevated in the high-latitude trough, but it is not in the mid-latitude trough (Rodger et al., 1992).

The presence of high-latitude troughs was initially identified from satellite observations at the early space age. From the measurements of the critical (plasma) frequency of the F region from the Canadian Alouette 1 satellite (launched in 1962), Muldrew (1965) identified plasma depletions at mid and high latitudes and named the depletions at middle latitudes (now known as mid-latitude trough) "main trough" and the depletions at high latitudes "high-latitude trough". Subsequently, a series of satellites were launched during the period of 1964–1972 by the United States under the Orbiting Geophysical Observatory (OGO) program. The understanding of the generation mechanisms of high-latitude troughs advanced through analysis of ion composition data from OGO-6 (launched in 1969) observations. In these observations, high-latitude troughs were characterized by depletions in atomic ions (O^+ and H^+) and enhancement in molecular ions (NO^+, $O_2{}^+$, and $N_2{}^+$) (Grebowsky et al., 1983; Taylor et al., 1975). The occurrence statistics of high-latitude troughs, derived from the OGO-6 observations at altitudes between 400 and 1,100 km in 1969–1970, revealed the development of high-latitude troughs at any local time in the vicinity of an auroral oval (Grebowsky et al., 1983). Taylor et al. (1975) suggested soft electron precipitation as the cause of plasma depletions at high-latitude troughs; the heating of the atmosphere by electron precipitation increases the O^+ loss rate by increasing the molecular gas number density in the F region and vibrationally excited N_2. However, the formation of sharp boundaries of high-latitude troughs required an additional process, and Grebowsky et al. (1983) suggested the trough formation by the enhanced dissociative recombination rate associated with high-speed plasma convection. Recent studies (Karpachev, 2022a, 2022b, 2023), investigated the conditions for the development of high-latitude troughs under midnight, morning, evening, and noon conditions using the electron concentration data from the Challenging Minisatellite Payload (CHAMP) satellite. Following these studies, two types of high-latitude troughs develop. One type reveals the formation of wide poleward walls by particle precipitations on the poleward edge of the auroral oval. The other type, observed inside the auroral oval, is not associated with particle precipitations but with a narrow band of rapid plasma drift.

The observations of the European Incoherent Scatter Scientific Association (EISCAT) radar enriched our understanding of the physical processes underlying high-latitude troughs. Common features at high-latitude troughs identified from EISCAT observations during different periods are enhancements in ion temperature, minor changes in electron temperature, outward field-aligned plasma flow, and strong horizontal plasma convection (Jones et al., 1990; Williams & Jain, 1986; Winser et al., 1986). Based on new findings from EISCAT observations, these studies suggested the significance of field-aligned plasma outflow, in conjunction with dissociative recombination, in the formation of high-latitude troughs. The Joule heating of the auroral *E* region by strong electric fields drives upward neutral winds, instigating dissociative recombination in the F region. Additionally, the rise in ion temperature contributes to plasma outflow through diffusion. These processes collectively elucidate the creation of a distinct depletion boundary within high-latitude troughs.

Synthesizing earlier studies that rely on OGO-6, CHAMP, and EISCAT observations, the heating of the atmosphere by high-speed plasma convection and particle precipitation plays a critical role in the formation of high-latitude troughs within confined regions (Jones et al., 1990; Rodger et al., 1992). However, an important feature identified from subsequent studies is the presence of downward field-aligned currents (FACs) at the locations of high-latitude troughs (Ishida et al., 2014; Vanhamäki et al., 2016; Zou et al., 2013). Numerical simulations show that downward FACs associated with electron outflows are an effective process for evacuating ionospheric plasma (Doe et al., 1995; Karlsson et al., 2007). Zou et al. (2013) suggested that the co-location of high-latitude troughs and downward FACs can be understood as an integral part of the substorm current system.

This study investigates the distribution and generation mechanisms of high-latitude troughs by analyzing Swarm-A observations from May to August 2014. This is the period during which the Swarm measurements of the plasma density, ionospheric radial current (IRC), electron temperature, and especially 3-dimensional ion velocity are available. Previous studies have inferred FACs from the measurements of plasma motions (Ishida et al., 2014;

Vanhamäki et al., 2016; Voiculescu et al., 2016; Zou et al., 2013) and magnetic perturbations (Vanhamäki et al., 2016; Yang et al., 2019). Swarm observations provide FAC information via level 2 IRC data derived from magnetometer measurements. The simultaneous observations of plasma density, plasma convection, and FACs provide a unique opportunity to examine the roles of plasma motion and FACs in the generation of high-latitude troughs. The IRC data are also valuable for the distinction of mid- and high-latitude troughs. Yang et al. (2019) investigated the relationship among the electron density, FAC, and plasma motion at high latitudes in the Southern Hemisphere using their mean values derived from Swarm-A data in 2013–2018. However, our study manually processes Swarm data from individual orbits to identify high-latitude troughs for following reasons. First, the analysis of individual events allows for a clearer demonstration of the causal relationship among different parameters. Because the occurrence rate of high-latitude troughs is low (<20%), mean parameter values may not precisely represent trough characteristics. Second, the mid- and high-latitude troughs are difficult to distinguish from the distribution of the mean density. From mean density plots in Yang et al. (2019) the mid- and high-latitude troughs are distinguishable only around postmidnight. Third, the characteristics of high-latitude troughs can be contaminated by those of mid-latitude troughs when mean values are used because high-latitude troughs are weak features occurring less frequently compared with mid-latitude troughs.

2. Data Set

The Swarm spacecraft, consisting of three identical satellites (A, B, and C), were launched in November 2013 with the primary goal of studying the Earth's magnetic field. This study uses the Swarm-A (altitude: ~460 km, inclination: 87.4°) observations of the electron density and temperature by Langmuir Probes (LP), ion drift velocity by Thermal Ion Imager (TII), and IRC by Vector Field Magnetometer (VFM). The cadence of density and temperature data is 2 Hz, and the cadence of IRC data is 1 Hz. The IRC data in the Swarm dataset is derived by applying the Ampere's law to measurements of magnetic field perturbations. To enhance data smoothness, a Savitzky-Golay filter (Savitzky & Golay, 1964) with 7-s time window is applied to all parameters. Because the IRC data show large fluctuations even after the filtering, an 11-s average of the filtered data is employed for the IRC analysis. The simultaneous observations of the plasma density, 3-dimensionl plasma velocity, IRC, and electron temperature by Swarm are limited to the timeframe of May–August in 2014. This period covers only one season, but these observations provide a rare opportunity to examine the distribution and generation mechanisms of the high-latitude trough during both summer (Northern Hemisphere) and winter (Southern Hemisphere).

The detection of the high-latitude trough from satellite observations is not straightforward because irregularities occur at anytime at high latitudes. To facilitate the high-latitude trough detection, Swarm-A orbits are divided into four segments: ascending and descending orbits for each hemisphere. The detection threshold of the high-latitude trough is set as a density depletion exceeding 40% compared to the mean density within ±60°–85° magnetic latitudes (MLAT). This 40% threshold is determined on the basis of our experimentation with various thresholds. After the automated detecting of candidate high-latitude troughs, manual verification is conducted to confirm actual events. The criteria for an authentic high-latitude trough are: (a) a density minimum present within ±60°–85° MLAT, (b) a trough-like density depletion structure, and (c) a location poleward of the equatorward auroral boundary.

Because mid- and high-latitude troughs develop at close latitudes, distinguishing between these troughs relies on their positioning relative to the auroral oval. Our study determines the auroral boundary using Swarm IRC data. To validate the IRC-based auroral boundary, we use the measurements of electron energy flux by the Special Sensor for Precipitating Particles version 4 (SSJ4) on board the Defense Meteorological Satellite Program (DMSP) F19, along with far ultraviolet emission data from the Special Sensor Ultraviolet Spectrographic Imager (SSUSI) on board the DMSP F17.

3. Observational Results

One of the distinguishing characteristics of an auroral oval is the presence of strong currents, and the auroral boundary has been determined from the measurements of currents (Chen et al., 2003; Milan et al., 2017). Karpachev (2019, 2022a, 2022b, 2023) classified troughs into mid- and high-latitude troughs from satellite observations using the auroral boundary obtained from an empirical model. However, the auroral boundary is variable with geomagnetic activity. In this study, we determine the auroral boundary for each orbit using the IRC data, recognizing that the actual auroral boundaries can differ from the model-generated ones. To assess the auroral

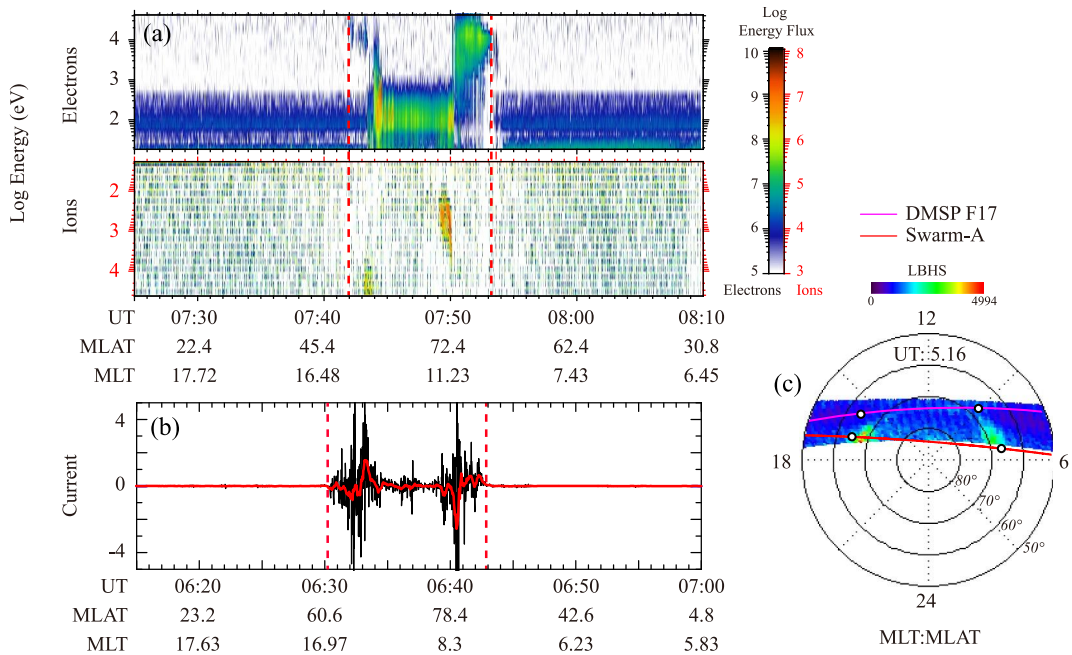

Figure 1. Comparison of the auroral oval boundaries determined by electron energy flux, IRC, and far ultraviolet emission for the observations on 12 July 2014. (a) Electron and ion energy fluxes observed by DMSP F19/SSJ4. (b) IRC data from Swarm-A. The red solid line represents an 11-s average of the IRC data. (c) LBHS emission from DMSP F17/SSUSI. The pink and red lines are the orbital trajectories of DMSP F19 and Swarm-A satellites. The white dots on the trajectories indicate the equatorial boundaries identified along those orbits.

boundaries determined from the Swarm IRC data, we compare the Swarm-A IRC data with the observations of other parameters by DMSP on 12 July 2014. Figure 1 presents (a) electron and ion energy fluxes from DMSP F19/SSJ4, (b) Swarm-A IRC, and (c) Lyman-Birge-Hopfield short (LBHS, 141.0–152.8 nm) emission from DMSP F17/SSUSI. The Kp and Ap indices around the time of these observations were 2 and 7, respectively. Radially outward IRCs have positive values. The equatorward boundary of the auroral oval is indicated by dashed red lines in Figures 1a and 1b, and these locations are marked by white dots on the satellite orbits in Figure 1c. About an hour difference exists among the three observations, but the location of the auroral oval remains consistent during this period. Figure 1c reveals a good alignment of the equatorward auroral boundaries as identified by electron energy flux, IRC, and LBHS emission.

Figure 2 shows the Swarm-A observations of plasma density, IRC, electron temperature, horizontal plasma velocity, and MLT and MLAT along the orbit in the (a–e) Northern and (f–j) Southern Hemispheres on 12 July 2014. The horizontal velocity is the velocity perpendicular to the satellite orbit. As Swarm-A has a polar orbit, the horizontal velocity is close to the zonal velocity. In the Northern Hemisphere, a trough feature appears at high latitudes around 06 MLT. Inside the trough, IRCs values exhibit fluctuations, electron temperature experiences a sharp increase near the trough's center, and the plasma motion is sunward (eastward) with a peak velocity of ~2,000 m/s. This trough is interpreted as a high-latitude trough because it is located poleward of the auroral boundary (vertical green line in Figure 2b).

In the Southern Hemisphere, two trough features appear. The trough indicated by the letter "A" is detected equatorward of the auroral boundary, and the trough indicated by the letter "B" is detected poleward of the auroral boundary. Therefore, trough A is interpreted as a mid-latitude trough, and trough B is interpreted as a high-latitude trough. The characteristics of trough B are similar to those of the trough detected in the Northern Hemisphere, showing density and IRC fluctuations, electron temperature enhancements, and a strong sunward plasma flow. In addition to the location relative to the auroral boundary, the density and IRC fluctuations and plasma motion are the distinguishing characteristics of the mid- and high-latitude troughs. A consistent feature in troughs A and B is the enhancement in the electron temperature. The high electron temperature at both troughs is discussed later.

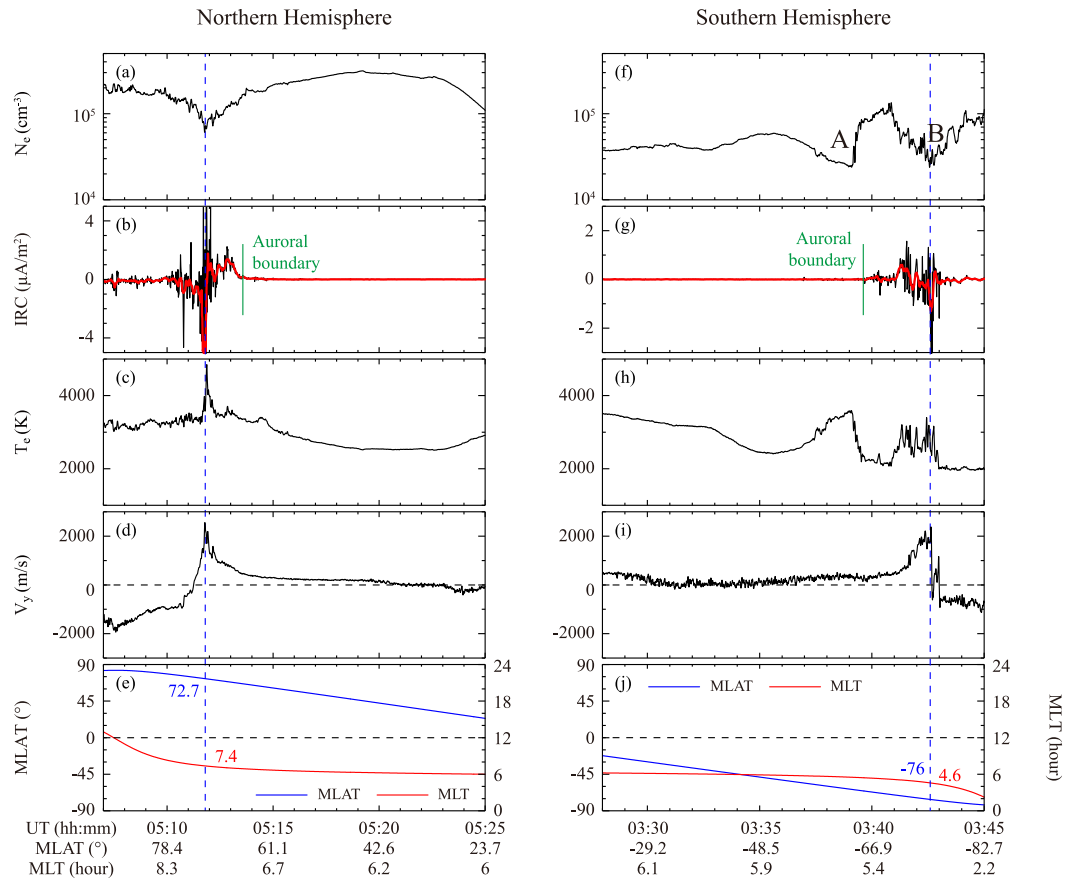

Figure 2. Examples of high-latitude troughs detected by Swarm-A in the Northern Hemisphere on 12 July 2014 (a–e) and in the Southern Hemisphere on 7 July 2014 (f–j) (a and f) Electron density (Ne) (b and g) IRC. The red solid line represents an 11-s average of the IRC data (c and h) Electron temperature (Te) (d and i) Horizontal ion velocity (Vy) (e and j) Magnetic latitude (MLAT) and magnetic local time (MLT) of Swarm-A orbit. Vertical dashed lines indicate the epochs of high-latitude troughs.

From the Swarm-A data during May–August in 2014, a total of 394 high-latitude trough events have been identified. Among these events, 244 and 150 events occurred in the Northern (summer) and Southern (winter) Hemispheres, respectively. The hemispheric difference in the event numbers suggests a potential preference for high-latitude trough occurrence in the summer hemisphere. The distribution and occurrence rate of high-latitude troughs are shown in Figure 3 (a and (b) MLAT and MLT distributions (d and (e) event count (vertical bars) and occurrence rate (black dots and lines) as a function of MLT, and (g and (h) Swarm-A orbit segment count in the (left) Northern and (right) Southern Hemispheres. Figures 3a and 3b show the occurrence of high-latitude troughs poleward of 60° magnetic latitudes. In general, the stronger the geomagnetic activity, the troughs appear to be located at lower latitudes. Troughs are detected at all MLTs, but they occur more frequently between 00 and 12 MLT in the Northern Hemisphere and around 18 MLT in the Southern Hemisphere. The low occurrence rate (<15%) indicates that high-latitude troughs are occasional phenomena occurring under specific conditions. The combined events of the Northern and Southern Hemispheres are shown in Figure 3c–3i.

In all high-latitude trough events identified in Figure 3 we have observed the presence of high-speed plasma motions within the troughs. Through orbit-by-orbit manual examination of the data, we have also noticed a more frequent occurrence of troughs under inward (downward) IRC conditions, with troughs being rare under outward (upward) IRC conditions. To gain insight into the mean behavior of physical parameters within these troughs, we conduct a superposed epoch analysis. The results at different MLT sectors in both hemispheres are shown in Figure 4 (a–d) plasma density after background subtraction (e–h) plasma velocity (i–l) electron temperature, and (m–p) IRC. The epoch corresponds to the time of the density minimum for each trough. The plots illustrate the median (red) and quartile (blue) values of the parameters within ±2 min centered at the epoch. For the density, the

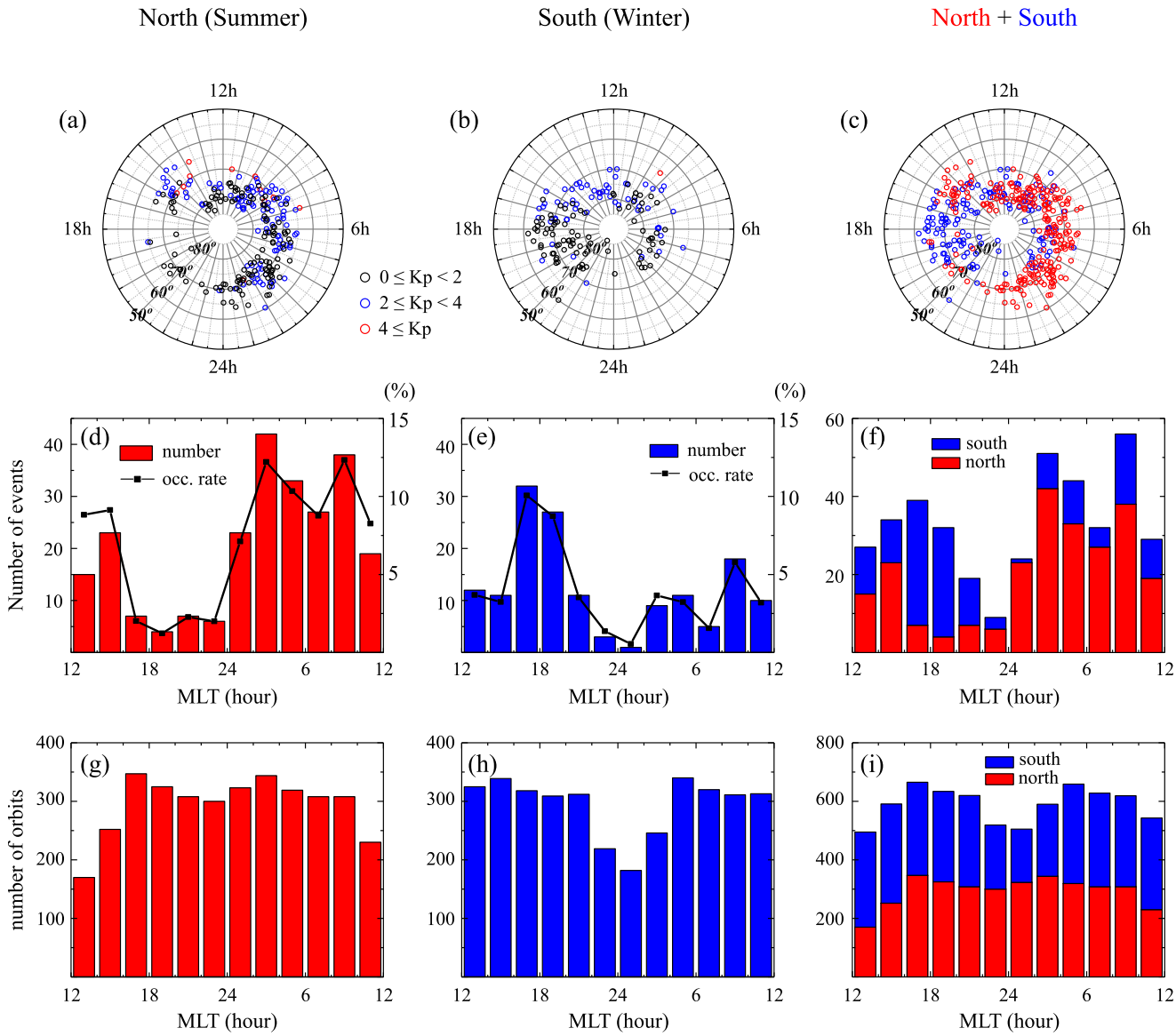

Figure 3. High-latitude trough distributions derived from the Swarm-A data during the period from May–August 2014 (a) and (b) Trough distributions in the MLT: MLAT coordinates in the Northern and Southern Hemispheres. Troughs are divided into weak ($0 \le Kp < 2$), medium ($2 \le Kp < 4$), and strong ($4 \le Kp$) by Kp value, which is the geomagnetic activity index (d) and (e) Distributions of event count (histogram) and event occurrence rate (black dots) as a function of MLT in the Northern and Southern Hemispheres (g) and (h) Number of Swarm-A orbit segments in the Northern and Southern Hemispheres. (c) A combination of (a) and (b). Red and blue circles represent troughs in the northern and southern hemispheres, respectively. (f) A combination of (d) and (e). Red and blue histograms represent events in the northern and southern hemispheres, respectively. (i) A combination of (g) and (h). Red and blue histograms represent number of Swarm-A orbit segments in the northern and southern hemispheres, respectively.

epoch analysis is conducted after subtracting the mean density because of the large variation range of the background density. The epoch analysis is conducted for trough events occurring at 03–09 MLT (dawn) and 15–21 MLT (dusk), as the large-scale FAC direction is difficult to determine around noon and midnight. In the velocity and IRC plots, positive values represent eastward velocity and radially outward IRC.

The trough appears to be more pronounced in the Northern (summer) Hemisphere than in the Southern (winter) Hemisphere. A part of this hemispheric difference can be attributed to the higher background density and Joule heating rate during summer; the decrease in electron density caused by enhanced chemical reactions becomes pronounced under the conditions of significant Joule heating and background density. For all cases, the epochs of the density and velocity coincide. This observation provides strong evidence of the significant role of plasma

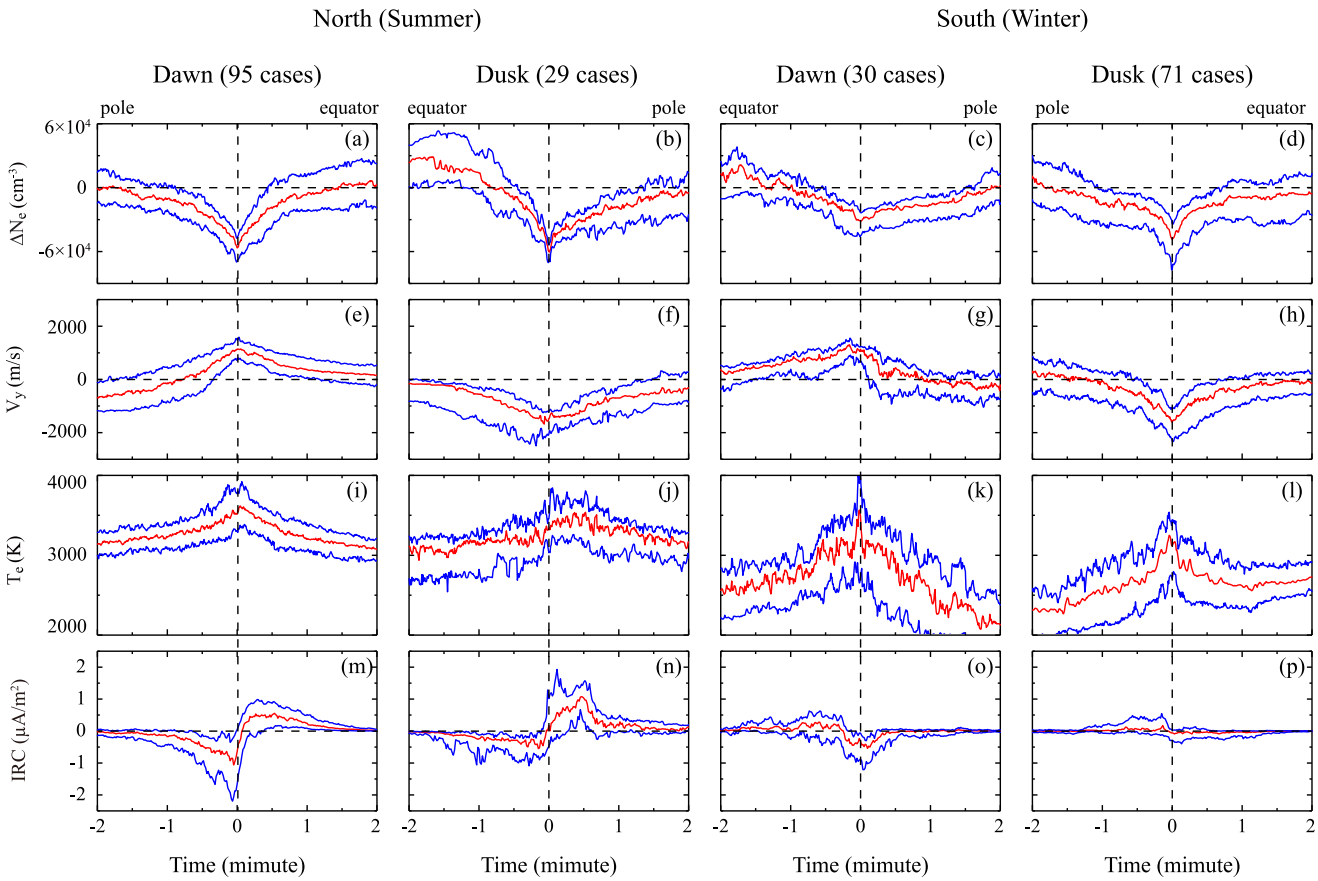

Figure 4. Superposed epoch analysis results of high-latitude trough parameters for four cases: dawn and dusk in the Northern and Southern Hemispheres (a–d) Electron density variation obtained after subtraction of the mean density (e–h) Horizontal ion velocity (i–l) Electron temperature (m–p) IRC. The epoch analysis is conducted using the data within 4-min intervals centered at the epoch of the density. In all plots, red lines represent median values and blue lines represent quartile values.

motion in the trough formation. However, IRC does not show consistent behavior. Similar to velocity, the epochs of electron temperature agree with density epochs. The elevated electron temperature in the troughs is attributed to their reciprocal relationship, as discussed later. In the Northern Hemisphere, IRC direction transitions are observed near the epoch at both dawn and dusk. At dawn (Figure 4m), IRC is directed downward and upward at the poleward and equatorward sides, respectively, over an auroral oval. This IRC variation with latitude corresponds to orientations of Region 1 and Region 2 FACs at dawn (Iijima & Potemra, 1978). The IRC direction transitions at dusk (Figure 4n) are also aligned with the established FAC directions. A noteworthy observation from Figure 4m is a slight shift in the epoch location toward downward IRC. In other words, IRC is downward at the density epoch. The downward IRC at the density epoch is also observed at dawn in the Southern Hemisphere (Figure 4o). At dusk in both hemispheres (Figures 4n and 4p), the IRC direction is near zero at the density epoch.

The statistical results in Figure 4 indicate that the preferred condition for high-latitude trough development is when FAC is downward or absent. The Swarm observations on 2 Aug 2014 in Figure 5 provide further insight into the role of FACs in high-latitude trough generation. In Figure 5a, two distinct trough features appear over the auroral oval. Trough A is detected around 15 MLT and trough B is detected around 05 MLT. Trough B exhibits a significantly more plasma depletion compared with Trough A, despite Trough A displaying more pronounced enhancements in electron temperature and ion velocity relative to the background (Figures 5c and 5d). Consequently, the difference of trough intensity between the two events does not appear to stem from differences in frictional heating. Upon comparing IRCs within the trough (Figure 5b), the IRC around the Trough A epoch has a large upward component, whereas the IRC around the Trough B epoch has a large downward component. While the instantaneous observations of a few physical parameters may not fully elucidate the formation process of these two troughs, the relationship between the trough intensity and IRC direction illustrated in this example aligns with the statistical results shown in Figure 4.

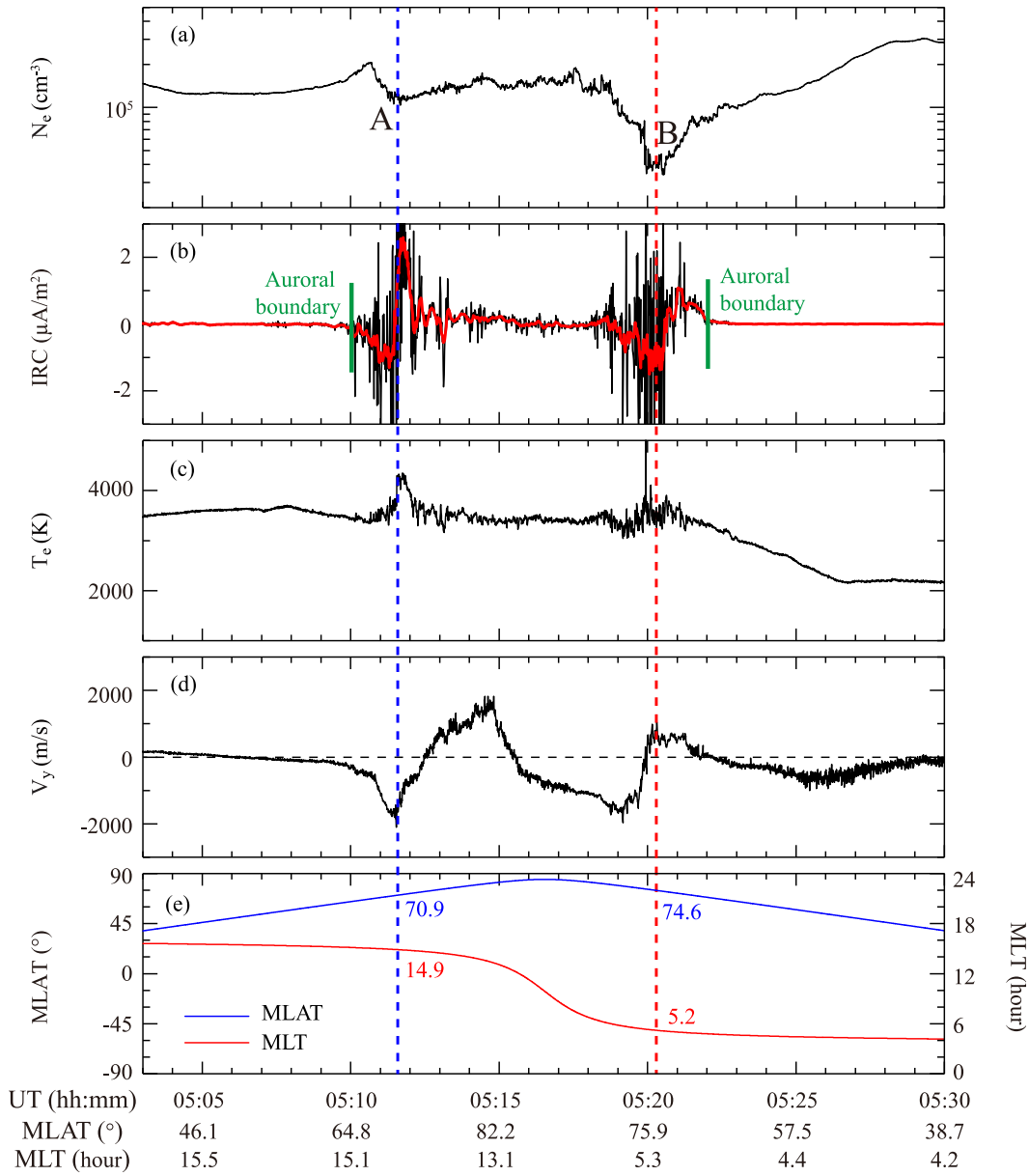

Figure 5. Comparison of two high-latitude troughs with different strengths observed on 2 August 2014 by Swarm-A. (a) Electron density. (b) IRC. The red solid line represents an 11-s average of the IRC data. (c) Electron temperature. (d) Horizontal ion velocity. (e) Magnetic latitude and local time of Swarm-A orbit. The vertical dashed blue and red lines indicate the epochs of the troughs at dusk (a) and dawn (b), respectively.

4. Discussion

High-speed plasma convection causes atmospheric frictional heating by ion-neutral collisions. This atmospheric heating, in turn, facilitates O^+ loss through chemical reactions with O_2 and N_2, resulting in plasma depletions. Many studies have proposed that the formation of high-latitude troughs is a consequence of these processes (Grebowsky et al., 1983; Jones et al., 1990; Rodger et al., 1992; Vanhamäki et al., 2016; Voiculescu et al., 2016; Williams & Jain, 1986; Winser et al., 1986). However, most of these studies were based on case studies of a limited number of events. In contrast, our study examined 396 high-latitude trough events and derived their average characteristics. From all these events, we have identified the development of troughs under high-speed plasma convection. This observation is consistent with the coincidence of the epochs of plasma density and velocity. All the trough events that we examined are characterized by high plasma velocity, and therefore, these

events belong to high-latitude trough 2 (HLT2), following the classification by Karpachev (2022a, 2022b). Electron outflow (or downward FAC) may contribute to the development of high-latitude troughs, but high-speed plasma convection is considered to play the primary role because troughs are detected even in the absence of downward FAC.

The electron outflow has also been suggested as a contributing factor to the high-latitude trough formation (Doe et al., 1993, 1995; Ishida et al., 2014; Karlsson et al., 2007; Vanhamäki et al., 2016; Zou et al., 2013). The electron outflow corresponds to downward FACs, and numerical simulations show that downward FACs can induce a significant density cavity more rapidly than dissociative recombination (Doe et al., 1995). Zou et al. (2013) utilized ground-based magnetometer measurements to deduce FACs and reported the coincident occurrence of strong plasma convection and plasma depletion at locations of downward FACs. Applying the Kamide-Richmond-Matsushita method (Kamide et al., 1981) to EISCAT's two-dimensional conductance data, Vanhamäki et al. (2016) derived ionospheric electric fields and FACs. Based on the case study of the event on 24–25 June 2003, Vanhamäki et al. (2016) suggested an evolution scenario of the high-latitude trough in the morning sector. According to this scenario, downward FACs initially create a trough poleward of the auroral oval by evacuating the F region plasma. This trough is intensified by dissociative recombination as it moves to lower latitudes and collocates with the westward electrojet. The trough is refilled through photoionization as sunrise approaches. Our observations support the role of FACs in the formation of high-latitude troughs. As shown in Figure 3, high-latitude troughs occur more frequently at dawn and dusk sectors than at noon and midnight sectors. This distribution bears similarity to the distribution of FACs, which display longitudinally extended bands centered at dawn and dusk (Iijima & Potemra, 1978). The prevalent detection of troughs under downward IRC conditions, coupled with their rarity under upward IRC conditions, further supports the role of FACs.

Ishida et al. (2014) derived the distribution of high-latitude troughs in the Northern Hemisphere by analyzing the EISCAT observations in 1982–2011. Their results show the high occurrence rate of high-latitude troughs in the morning sector in summer months (June solstice). This observation agrees with our observations in the Northern Hemisphere that show a much high occurrence rate of high-latitude troughs in the morning sector (00–12 MLT) than in the evening sector (12–00 MLT) (Figures 3a and 3c). In the winter season, according to the observations of Ishida et al. (2014), the occurrence rate of high-latitude troughs peaks around 04 and 17 MLTs and has a minimum around 21 MLT. As Swarm's winter observations are only available in the Southern Hemisphere, we compare our observations around the June solstice in the Southern Hemisphere with the EISCAT observations around December solstice in the Northern Hemisphere. Our Figures 3b and 3d show the peak occurrence rate of high-latitude troughs around 17 MLT and a minimum occurrence rate around midnight. However, the occurrence rate around 04 MLT is not as pronounced as that around 17 MLT in our observations. This difference may reflect hemispheric differences in trough behavior. The assessment of the seasonal behavior of the trough in opposite hemispheres requires observations in both hemispheres for a longer period. In the observations of Ishida et al. (2014), high-latitude troughs rarely occur around noon. However, as Figures 3a and 3b reveal, high-latitude troughs are not infrequent phenomena around noon in our observations. This difference is seen to be partly linked to the occurrence of noontime high-latitude troughs at higher MLAT than during other times. In our observations, they appear mostly poleward of 70° MLAT, whereas EISCAT data are unavailable poleward of 72° MLAT. The generation of troughs at the cusp region can be understood in connection with atmospheric heating caused by soft particle precipitation. The effect of atmospheric heating on plasma density has been identified in the *E* region (Voiculescu et al., 2016). Additionally, enhanced chemical reactions due to the Joule heating associated with large electric fields maximize at the equatorward edge of the cusp, leading to the net depletion in total electron content and plasma density measurements (Basinska et al., 1987). Atmospheric heating within the cusp region can be one of the reasons for the higher occurrence rate of high-latitude troughs around noon compared to around midnight in our observations. Even though the auroral boundaries were determined using the IRC data according to the auroral boundary criteria applied in this study, some troughs can be located equatorward of the auroral region when cusp auroras occur around noon region where the current is very complex.

While Swarm electron temperature measurements have a certain level of uncertainty (Catapano et al., 2022; Lomidze et al., 2018, 2021), our statistical results reveal their mean behavior. Enhancements in electron temperature at high-latitude troughs is a consistent feature identified at any time in both hemispheres (Figure 4). In previous studies (Ma et al., 2000; Zou et al., 2013), the electron temperature was one of the distinguishing parameters between mid- and high-latitude troughs. The electron temperature at mid-latitude troughs is higher than that of ambient electron because of the low electron density at troughs. This reciprocal relationship between the

electron density and temperature at mid-latitude troughs is evident from the observations in Figures 2f and 2h. In these observations, the electron temperature in Trough A (mid-latitude trough) is about 1000 K higher than that of the background. The reciprocal relationship between electron density and temperature is explained by the increase in electron energy loss through collisions with ions as plasma density increases. For high-latitude troughs, different studies have reported different behaviors of electron temperature. Vanhamäki et al. (2016) and Voiculescu et al. (2016) reported an absence of notable change in electron temperature at high-latitude troughs, while Zou et al. (2013) even reported a decrease in electron temperature at a high-latitude trough at F region height. Our observations differ from these observations. In our observations, the electron temperature is at its highest at the center of high-latitude troughs. We interpret this as indicating that the reciprocal relationship between electron density and temperature is effective not only in mid-latitude troughs but also in high-latitude troughs.

Our results align with previous research from the point of view of high-speed plasma convection and downward current. But there are some differences from Yang et al. (2019) which used the Swarm same as we did. They average the 4-year accumulated electron density, ion drift, and FAC data and confirm the production of the high-latitude trough at different local time regions. They suggested that the production of high-latitude troughs is caused by plasma stagnation and downward current. The methodological problem may cause a discrepancy in the ion velocity pattern. The mid-latitude trough is a quite steady phenomenon produced in the non-sunlit region where the convection and corotation are opposite. Many studies used accumulated methods to research mid-latitude troughs because they are a phenomenon that lasts a relatively long time and is generated frequently (He et al., 2011; Lee et al., 2011). However, as Rodger et al. (1992) mentioned, high-latitude troughs are relatively short-lasting events that survive only 4–8 hr because they are located in the dynamic region rather than mid-latitude troughs. As we can see in Figure 3, high-latitude troughs are located variable in the convection region, changing by geomagnetic and interplanetary magnetic field (IMF) conditions. FACs also have a variable position in the ionosphere, changing by those geomagnetic and IMF conditions. In addition, as shown in Figure 3, the occurrence rate of high-latitude troughs is only up to 12%, so the accumulated method may not suitable for the high-latitude trough research. Since the high-latitude trough is produced in the dynamic regions continuously generating photoionization, we used the various ionospheric parameters simultaneously.

5. Conclusions

We investigated the distribution and formation mechanisms of high-latitude ionization troughs by analyzing the measurements of electron density and temperature, horizontal ion velocity, and IRC by Swarm-A during the period from May to August in 2014. The results obtained from Swarm-A observations clearly indicate the crucial role of high-speed plasma streams in the formation of high-latitude troughs. Although FACs are not a primary driving factor, it is evident that downward FACs (outward electron flow) contribute to the generation of high-latitude troughs. The behavior of electron temperature at high-latitude troughs has been inconsistent in different studies. However, our observations consistently show an enhancement of electron temperature at troughs. The limited duration of Swarm observations over only 4 months restricts a comprehensive understanding of the behavior and sources of high-latitude troughs. The occurrence rate of high-latitude troughs in the Northern and Southern Hemispheres, as well as their distribution as a function of magnetic local times derived from the data during this period, may not represent the general behavior of high-latitude troughs. Our results, which based on data around the June solstice in 2014, can differ from those obtained from observations during other seasons or different years. Nonetheless, our study has identified key properties of high-latitude troughs that were observed by radars.

Data Availability Statement

Plasma density and electron temperature data from Swarm satellites are available from Swarm-LP (2024). 3-Dimensional ion velocity and ionospheric radial current data are available from Swarm-TII (2024) and Swarm-VFM (2024), respectively.

Acknowledgments
This work was supported by basic research funding from the Korea Astronomy and Space Science Institute (KASI) (KASI2024185002). H. Kil acknowledges support from NSF-AGS2029840 and NASA-NNH19ZDA001N. The work of K.-H. Kim was supported by NRF-2023R1A2C1002994.

References

Aa, E., Zou, S., Erickson, P. J., Zhang, S.-R., & Liu, S. (2020). Statistical analysis of the main ionospheric trough using Swarm in situ measurements. *Journal of Geophysical Research: Space Physics*, *125*(3), e2019JA027583. https://doi.org/10.1029/2019JA027583

Anderson, P. C., Johnston, W. R., & Goldstein, J. (2008). Observations of the ionospheric projection of the plasmapause. *Geophysical Research Letters*, *35*(15), L15110. https://doi.org/10.1029/2008GL033978

Basinska, E. M., Burke, W. J., Basu, S., Rich, F. J., & Fougere, P. F. (1987). Low-frequency modulation of plasmas and soft electron precipitation near dayside cusp. *Journal of Geophysical Research*, *92*(4), 3304–3314. https://doi.org/10.1029/JA092iA04p03304

Catapano, F., Buchert, S. C., Qamili, E., Nilsson, T., Bouffard, J., Siemes, C., et al. (2022). Swarm Langmuir probes' data quality validation and future improvements. *Geosci. Instrum. Method. Data Syst.*, *11*(1), 149–162. https://doi.org/10.5194/gi-11-149-2022

Chen, G. X., Xu, W. Y., Wei, Z. G., Ahn, B. H., & Kamide, Y. (2003). Auroral electrojet oval. *Earth Planets and Space*, *55*(5), 255–261. https://doi.org/10.1186/BF03351757

Doe, R. A., Mendillo, M., Vickrey, J. F., Zanetti, L. J., & Eastes, R. W. (1993). Observations of nightside auroral cavities. *Journal of Geophysical Research*, *98*(A1), 293–310. https://doi.org/10.1029/92JA02004

Doe, R. A., Vickrey, J. F., & Mendillo, M. (1995). Electrodynamic model for the formation of auroral ionospheric cavities. *Journal of Geophysical Research*, *100*(A6), 9683–9696. https://doi.org/10.1029/95JA00001

Dudeney, J., Jarvis, M., Kressman, R., Pinnock, M., Rodger, A. S., & Wright, K. H. (1982). Ionospheric troughs in Antarctica. *Nature*, *295*(5847), 307–308. https://doi.org/10.1038/295307a0

Fu, H. S., Tu, J., Cao, J. B., Song, P., Reinisch, B. W., Gallagher, D. L., & Yang, B. (2010). IMAGE and DMSP observations of a density trough inside the plasmasphere. *Journal of Geophysical Research*, *115*(A7), A07227. https://doi.org/10.1029/2009JA01510

Grebowsky, J. M., Chen, A. J., & Taylor, H. A. (1976). High-latitude troughs and the polar cap boundary. *Journal of Geophysical Research*, *81*(4), 690–694. https://doi.org/10.1029/JA081i004p00690

Grebowsky, J. M., Taylor, H. A., & Lindsay, J. M. (1983). Location and source of ionospheric high latitude troughs. *Planetary and Space Science*, *31*(1), 99–105. https://doi.org/10.1016/0032-0633(83)90034-X

Hanson, W. B., & Moffett, R. J. (1966). Lonization transport effects in the equatorial F region. *Journal of Geophysical Research*, *71*(23), 5559–5572. https://doi.org/10.1029/JZ071i023p05559

He, M., Liu, L., Wan, W., & Zhao, B. (2011). A study on the nighttime midlatitude ionospheric trough. *Journal of Geophysical Research*, *116*(A5), A05315. https://doi.org/10.1029/2010JA016252

Iijima, T., & Potemra, T. A. (1978). Large-scale characteristics of field-aligned currents associated with substorms. *Journal of Geophysical Research*, *83*(A2), 599–615. https://doi.org/10.1029/JA083iA02p00599

Ishida, T., Ogawa, Y., Kadokura, A., Hiraki, Y., & Häggström, I. (2014). Seasonal variation and solar activity dependence of the quiet-time ionospheric trough. *Journal of Geophysical Research: Space Physics*, *119*(8), 6774–6783. https://doi.org/10.1002/2014JA019996

Jones, G. O. L., Williams, P. J. S., Winser, K. J., & Lockwood, M. (1990). Characteristics of the high-latitude trough. *Advances in Space Research*, *10*(6), 191–196. https://doi.org/10.1016/0273-1177(90)90253-V

Kamide, Y., Richmond, A. D., & Matsushita, S. (1981). Estimation of ionospheric electric fields, ionospheric currents, and field-aligned currents from ground magnetic records. *Journal of Geophysical Research*, *86*(A2), 801–813. https://doi.org/10.1029/JA086iA02p00801

Karlsson, T., Brenning, N., Marghitu, O., Marklund, G., & Buchert, S. C. (2007). High-altitude signatures of ionospheric density depletions caused by field-aligned currents. *arXiv: Space Physics*, 1–11. https://doi.org/10.48550/arXiv.0704.1610

Karpachev, A. T. (2019). Variations in the winter troughs' position with local time, longitude, and solar activity in the Northern and Southern Hemispheres. *Journal of Geophysical Research: Space Physics*, *124*(10), 8039–8055. https://doi.org/10.1029/2019JA026631

Karpachev, A. T. (2022a). Advanced separation and classification of ionospheric troughs in midnight conditions. *Scientific Reports*, *12*(1), 13434. https://doi.org/10.1038/s41598-022-17591-4

Karpachev, A. T. (2022b). Advanced classification of ionospheric troughs in the morning and evening conditions. *Remote Sensing*, *14*(16), 4072. https://doi.org/10.3390/rs14164072

Karpachev, A. T. (2023). Structure of the high-latitude noon ionosphere of the southern hemisphere. *Remote Sensing*, *15*(14), 3649. https://doi.org/10.3390/rs15143649

Knudsen, W. C. (1974). Magnetospheric convection and the high-latitude F 2 ionosphere. *Journal of Geophysical Research*, *79*(7), 1046–1055. https://doi.org/10.1029/JA079i007p01046

Lee, I. T., Wang, W., Liu, J. Y., Chen, C. Y., & Lin, C. H. (2011). The ionospheric midlatitude trough observed by FORMOSAT-3/COSMIC during solar minimum. *Journal of Geophysical Research*, *116*(A6), A06311. https://doi.org/10.1029/2010JA015544

Lomidze, L., Burchill, J. K., Knudsen, D. J., & Huba, J. D. (2021). Estimation of ion temperature in the upper ionosphere along the Swarm satellite orbits. *Earth and Space Science*, *8*(11), e2021EA001925. https://doi.org/10.1029/2021EA001925

Lomidze, L., Knudsen, D. J., Burchill, J., Kouznetsov, A., & Buchert, S. C. (2018). Calibration and validation of Swarm plasma densities and electron temperatures using ground-based radars and satellite radio occultation measurements. *Radio Science*, *53*(1), 15–36. https://doi.org/10.1002/2017RS006415

Ma, S. Y., Liu, P., & Schlegel, K. (2000). EISCAT observation of a high-latitude ionization trough associated with a reversed westward plasma flow. *Geophysical Research Letters*, *27*(20), 3269–3272. https://doi.org/10.1029/2000GL000073

Milan, S. E., Clausen, L. B. N., Coxon, J. C., Carter, J. A., Walach, M. T., Laundal, K., et al. (2017). Overview of solar wind–magnetosphere–ionosphere–atmosphere coupling and the generation of magnetospheric currents. *Space Science Reviews*, *206*(1–4), 547–573. https://doi.org/10.1007/s11214-017-0333-0

Moffett, R. J., & Quegan, S. (1983). The mid-latitude trough in the electron concentration of the ionospheric F-layer: A review of observations and modelling. *Journal of Atmospheric and Terrestrial Physics*, *45*(5), 315–343. https://doi.org/10.1016/S0021-9169(83)80038-5

Muldrew, D. B. (1965). F-layer ionization troughs deduced from Alouette data. *Journal of Geophysical Research*, *70*(11), 2635–2650. https://doi.org/10.1029/JZ070i011p02635

Park, S., Kim, K.-H., Kil, H., Jee, G., Lee, D.-H., & Goldstein, J. (2012). The source of the steep plasma density gradient in middle latitudes during the 11–12 April 2001 storm. *Journal of Geophysical Research*, *117*(A5), A05313. https://doi.org/10.1029/2011JA017349

Rodger, A. S., Moffett, R. J., & Quegan, S. (1992). The role of ion drift in the formation of ionization troughs in the mid- and high-latitude ionosphere—A review. *Journal of Atmospheric and Terrestrial Physics*, *54*(1), 1–30. https://doi.org/10.1016/0021-9169(92)90082-V

Savitzky, A., & Golay, M. J. E. (1964). Smoothing and differentiation of data by simplified least squares procedures. *Analytical Chemistry*, *36*(8), 1627–1639. https://doi.org/10.1021/ac60214a047

Spiro, R. W., Heelis, R. A., & Hanson, W. B. (1978). Ion convection and the formation of the mid-latitude F region ionization trough. *Journal of Geophysical Research*, *83*(A9), 4255–4264. https://doi.org/10.1029/JA083iA09p04255

Swarm-LP. (2024). Measurements of plasma density and electron temperature data. [Dataset]. Retrieved from https://swarm-diss.eo.esa.int/#swarm%2FAdvanced%2FPlasma_Data%2F2_Hz_Langmuir_Probe_Extended_dataset

Swarm-TII. (2024). Measurements of 3-dimensional ion velocity data. [Dataset]. Retrieved from https://swarm-diss.eo.esa.int/#swarm%2FAdvanced%2FPlasma_Data%2F2_Hz_Ion_Drift_Density_and_Effective_Mass_dataset

Swarm-VFM. (2024). Measurements of ionospheric radial current data. [Dataset]. Retrieved from https://swarm-diss.eo.esa.int/#swarm%2FLevel2daily%2FEntire_mission_data%2FFAC%2FTMS

Taylor, H. A., Grebowsky, J. M., & Chen, A. J. (1975). Ion composition irregularities and ionosphere-plasmasphere coupling: Observations of a high latitude ion trough. *Journal of Atmospheric and Terrestrial Physics*, *37*(4), 613–623. https://doi.org/10.1016/0021-9169(75)90056-2

Vanhamäki, H., Aikio, A., Voiculescu, M., Juusola, L., Nygrén, T., & Kuula, R. (2016). Electrodynamic structure of the morning high-latitude trough region. *Journal of Geophysical Research: Space Physics*, *121*(3), 2669–2682. https://doi.org/10.1002/2015JA022021

Voiculescu, M., Nygrén, T., Aikio, A. T., Vanhamäki, H., & Pierrard, V. (2016). Postmidnight ionospheric troughs in summer at high latitudes. *Journal of Geophysical Research: Space Physics*, *121*(12), 12171–12185. https://doi.org/10.1002/2016JA023360

Voiculescu, M., Virtanen, I., & Nygrén, T. (2006). The F-region trough: Seasonal morphology and relation to interplanetary magnetic field. *Annales Geophysicae*, *24*(1), 173–185. https://doi.org/10.5194/angeo-24-173-2006

Werner, S., & Prölss, G. W. (1997). The position of the ionospheric trough as a function of local time and magnetic activity. *Advances in Space Research*, *20*(9), 1717–1722. https://doi.org/10.1016/S0273-1177(97)00578-4

Whalen, J. A. (1989). The daytime F layer trough and its relation to ionospheric-magnetospheric convection. *Journal of Geophysical Research*, *94*(A12), 17169–17184. https://doi.org/10.1029/JA094iA12p17169

Williams, P. J. S., & Jain, A. R. (1986). Observations of the high latitude trough using EISCAT. *Journal of Atmospheric and Terrestrial Physics*, *48*(5), 423–434. https://doi.org/10.1016/0021-9169(86)90119-4

Winser, K. J., Jones, G. O. L., & Williams, P. J. S. (1986). A quantitative study of the high latitude ionospheric trough using EISCAT's common programmes. *Journal of Atmospheric and Terrestrial Physics*, *48*(9–10), 893–904. https://doi.org/10.1016/0021-9169(86)90064-4

Yang, N., Le, H., & Liu, L. (2015). Statistical analysis of ionospheric mid-latitude trough over the Northern Hemisphere derived from GPS total electron content data. *Earth Planets and Space*, *67*(1), 196. https://doi.org/10.1186/s40623-015-0365-1

Yang, N., Yu, T., Le, H., Liu, L., Sun, Y.-Y., Xia, C., et al. (2019). The high-latitude trough in the Southern Hemisphere observed by Swarm-A satellite. *Journal of Geophysical Research: Space Physics*, *124*(11), 9475–9485. https://doi.org/10.1029/2019JA027169

Yizengaw, E., & Moldwin, M. B. (2005). The altitude extension of the mid-latitude trough and its correlation with plasmapause position. *Geophysical Research Letters*, *32*(9), L09105. https://doi.org/10.1029/2005GL022854

Yizengaw, E., Wei, H., Moldwin, M. B., Galvan, D., Mandrake, L., Mannucci, A., & Pi, X. (2005). The correlation between mid-latitude trough and the plasmapause. *Geophysical Research Letters*, *32*(10), L10102. https://doi.org/10.1029/2005GL022954

Zou, S., Moldwin, M. B., Nicolls, M. J., Ridley, A. J., Coster, A. J., Yizengaw, E., et al. (2013). Electrodynamics of the high-latitude trough: Its relationship with convection flows and field-aligned currents. *Journal of Geophysical Research: Space Physics*, *118*(5), 2565–2572. https://doi.org/10.1002/jgra.50120